

Aesthetic Surgery Journal

<http://aes.sagepub.com/>

TUNEL Assay to Characterize Acute Histopathological Injury Following Treatment With the Active and Deep FX Fractional Short-Pulse CO2 Devices

Jordan P. Farkas, James A. Richardson, Spencer A. Brown, Becca Ticker, Evan Walgama, Clint F. Burrus, John E. Hoopman, Fritz E. Barton and Jeffrey M. Kenkel
Aesthetic Surgery Journal 2010 30: 603
DOI: 10.1177/1090820X10380547

The online version of this article can be found at:
<http://aes.sagepub.com/content/30/4/603>

Published by:



<http://www.sagepublications.com>

On behalf of:



[American Society for Aesthetic Plastic Surgery](#)

Additional services and information for *Aesthetic Surgery Journal* can be found at:

Email Alerts: <http://aes.sagepub.com/cgi/alerts>

Subscriptions: <http://aes.sagepub.com/subscriptions>

Reprints: <http://www.sagepub.com/journalsReprints.nav>

Permissions: <http://www.sagepub.com/journalsPermissions.nav>

>> [Version of Record](#) - Sep 9, 2010

[What is This?](#)

TUNEL Assay to Characterize Acute Histopathological Injury Following Treatment With the Active and Deep FX Fractional Short-Pulse CO₂ Devices

Aesthetic Surgery Journal
30(4) 603–613
© 2010 The American Society for
Aesthetic Plastic Surgery, Inc.
Reprints and permission:
[http://www.sagepub.com/
journalsPermissions.nav](http://www.sagepub.com/journalsPermissions.nav)
DOI: 10.1177/1090820X10380547
www.aestheticsurgeryjournal.com


Jordan P. Farkas, MD; James A. Richardson, DVM, PhD;
Spencer A. Brown, PhD; Becca Ticker; Evan Walgama; Clint F. Burrus,
BA; John E. Hoopman; Fritz E. Barton, MD; and Jeffrey M. Kenkel, MD

Abstract

Background: This is a report of the histopathological evaluation of the acute damage profile in human skin following treatment with two novel short-pulsed fractional carbon dioxide resurfacing devices used independently and in combination *in vivo*.

Methods: The pannu of eight abdominoplasty patients were treated with either the Active FX, the Deep FX (Lumenis Ltd., Yokneum, Israel), or a combination of the two (Total FX) prior to the start of the excisional surgical procedure. Multiple combinations of energies, pulse widths, and densities were evaluated for each device. After surgical removal (two to five hours), each pannus was immediately biopsied and samples were processed for histopathological evaluation.

Results: The Active FX system resulted in extensive epidermal injury with wide shallow ablation craters that, at higher fluences, extended through the basement membrane of the epidermis into the papillary dermis. The Deep FX fractional treatment caused deep microcolumns of ablation penetrating up to 3 to 4 mm from the epidermal surface into the deep reticular dermis with a variable rim of coagulated collagen surrounding each ablation column.

Conclusions: The *in vivo* histopathological evaluation of these devices furthers our understanding of the fundamental laser/tissue interaction following treatment with each device independently and in combination.

Keywords

Ablative laser, CO₂, skin, resurfacing, histology

Accepted for publication July 14, 2010.

Fractional technology has restimulated interest in carbon dioxide laser resurfacing. The literature is replete with reports confirming the clinical efficacy of traditional carbon dioxide (CO₂) skin resurfacing; however, the impressive skin rejuvenation seen following these procedures came at the cost of considerable adverse events such as prolonged erythema, hypopigmentation, and scarring.¹⁻¹⁰

The excessive thermal injury previously seen with the traditional carbon dioxide treatments is avoided, theoretically, by fractionated laser injury. The fractional devices operate with an ultra-fast pulse of energy to produce tissue ablation and minimize heat deposition, decreasing the potential residual thermal damage to the surrounding uninjured skin.^{3,11-17} Fractional injury, in theory, is based on the damage and/or removal of microscopic portions of epidermis and disorganized elastotic collagen of the dermis to stimulate an accelerated healing response and replacement

of older, damaged collagen matrix with a new, organized, robust collagen matrix and a regenerated epidermal surface.^{18,19} Novel fractional ablative devices are marketed to induce neocollagenesis and collagen contracture with minimal posttreatment comorbidity and downtime. The science and mechanisms behind fractional wound healing remain poorly understood and continue to be topics of intense investigation and debate. Surprisingly, only a modest amount of objective scientific data are available in

From the University of Texas Southwestern Medical Center, Dallas, TX, USA.

Corresponding Author:

Dr. Jeffrey M. Kenkel, 1801 Inwood Drive, Dallas, Texas 75390.
E-mail: jeffrey.kenkel@utsouthwestern.edu.

Table 1. The Device Parameters Evaluated With the Active and Deep FX Systems

Device(s)	Energy Per Microbeam, mJ	Repetition Rate (AFX Only), Hz	Number of Pulses (DFX Only)	Density
Active FX	50-200	25-150	NA	1-6
Deep FX	2.5-35	NA	1, 2, 4	1-5
Combination (Active FX/Deep FX)	50, 70/ 15-25	100	2	3/2

NA, not applicable.

support of this exciting novel CO₂ technology in live human tissue.^{19,20}

Hantash and colleagues^{19,20} provided an excellent study with regard to the effect of fractional ablative CO₂ resurfacing on human forearm skin, incorporating histology throughout the wound-healing process over a three-month time interval. However, differences in the pattern of the injury with respect to alternative energies per pulse beam, pulse widths, number of passes, and densities for a given treatment still remain unclear.

This report evaluates the acute histopathological skin changes following in vivo treatment with the Active and Deep FX short-pulse CO₂ systems applied alone and in combination procedures on human abdominal skin with the immunofluorescent terminal deoxynucleotidyl transferase-mediated deoxyuridine triphosphate nick-end labeling (TUNEL) assay as a marker for irreversible cellular injury.²¹ Each device was evaluated at multiple clinical laser parameters (eg, energy per pulse, pulse width, repetition [rep] rate, density, and number of pulses).

METHODS

Eight healthy abdominoplasty patients of the senior author (JMK) were treated with either the Active FX, Deep FX (Lumenis Ltd., Yokneum, Israel), or a combination of the two (Total FX). One of the eight was treated with Deep FX followed immediately by Active FX. All patients in the study were Fitzpatrick skin phototypes I to IV. Skin types V to VI were excluded from the study. Three patients were treated with the Active FX alone, four were treated with the Deep FX alone, and one patient was treated with the Active FX system and then immediately afterward with the Deep FX device. The abdomen of each patient was treated just prior to the start of the surgical procedure. Each treatment parameter (energy, pulses, density, rep rate) evaluated was performed in triplicate on each participant, resulting in approximately 40 to 60 treatment areas per patient. Parameters evaluated for each device in the study are outlined in Table 1. The number of treatment spots varied slightly from patient to patient, depending on the amount of tissue planned for excision. Parameters were selected based on the clinical experiences of the senior author (JMK). The study was approved by the Institutional Review Board of the

University of Texas Southwestern Medical Center. Appropriate informed consent regarding all potential risks, objectives, and technical details were obtained from each participant.

All laser procedures were performed by a single surgeon (JMK). All patients were placed under general anesthesia by a board-certified anesthesiologist prior to treatment. The Active FX short-pulse CO₂ device contains a 1.2-mm spot size with a variable pulse width of <2 ms; it was calibrated with multiple energy settings ranging from 50 to 200 mJ and a repetition rate of 25 to 150 Hz (Table 1). All areas were treated with a single pass with a nonsequential computer pattern generator (CPG) density of 1 to 6. The Deep FX device employs a 0.12-mm spot size with a fixed pulse width (~250 μs). The repetition rate varies directly with the selected treatment energy. At a higher energy output, the repetition rate will decrease accordingly. The energies evaluated ranged from 2.5 to 35 mJ at single, double, and quadruple pulses. The energy delivered in relation to surface area of each device per microbeam varied by one order of magnitude of difference on account of the spot sizes (1.2 mm vs .12 mm). For example, the Active FX device at 150 mJ/cm² had approximately the equivalent energy/microbeam of the Deep FX device at 15 mJ/cm² (133 mJ/microbeam). The change in density for a given treatment correlated with the number of microbeams per treatment area.

Multiple pulsed treatments in this study were defined as multiple consecutive firings of the device without removing it from the treatment spot. For example, the double-pulsed treatments underwent consecutive firing of the device before moving the handpiece to the next treatment spot. Such a large range of energies was selected to define the potential damage at the maximum settings of each device. All areas were treated with a single pass at a CPG density of 1 to 5. The combination treatments consisted of sites treated with a single pass of the Active FX device, followed by a single-pass treatment of the Deep FX at the predetermined settings outlined in Table 1.

Punch biopsies (8 mm) were obtained from the treated sites following surgical excision of the pannus, approximately two to five hours (which was dependent on the duration of the abdominoplasty operation) following each laser treatment. Sections were placed in 10% neutral buffered formalin and then placed on a shaker for 24 hours. After rinsing in 70% ethanol solution, the biopsies were processed, embedded in paraffin, cut in serial longitudinal sections (4-6 μm), and mounted on poly-L-lysine slides. Multiple serial sections (10-15) of each specimen were processed to obtain accurate representation of the damage profile in each treatment sample.

Histopathological Evaluation

Hematoxylin and Eosin

Slides were stained with standard hematoxylin and eosin (H&E) protocol; unstained contiguous sections were stained with the immunofluorescent TUNEL method to

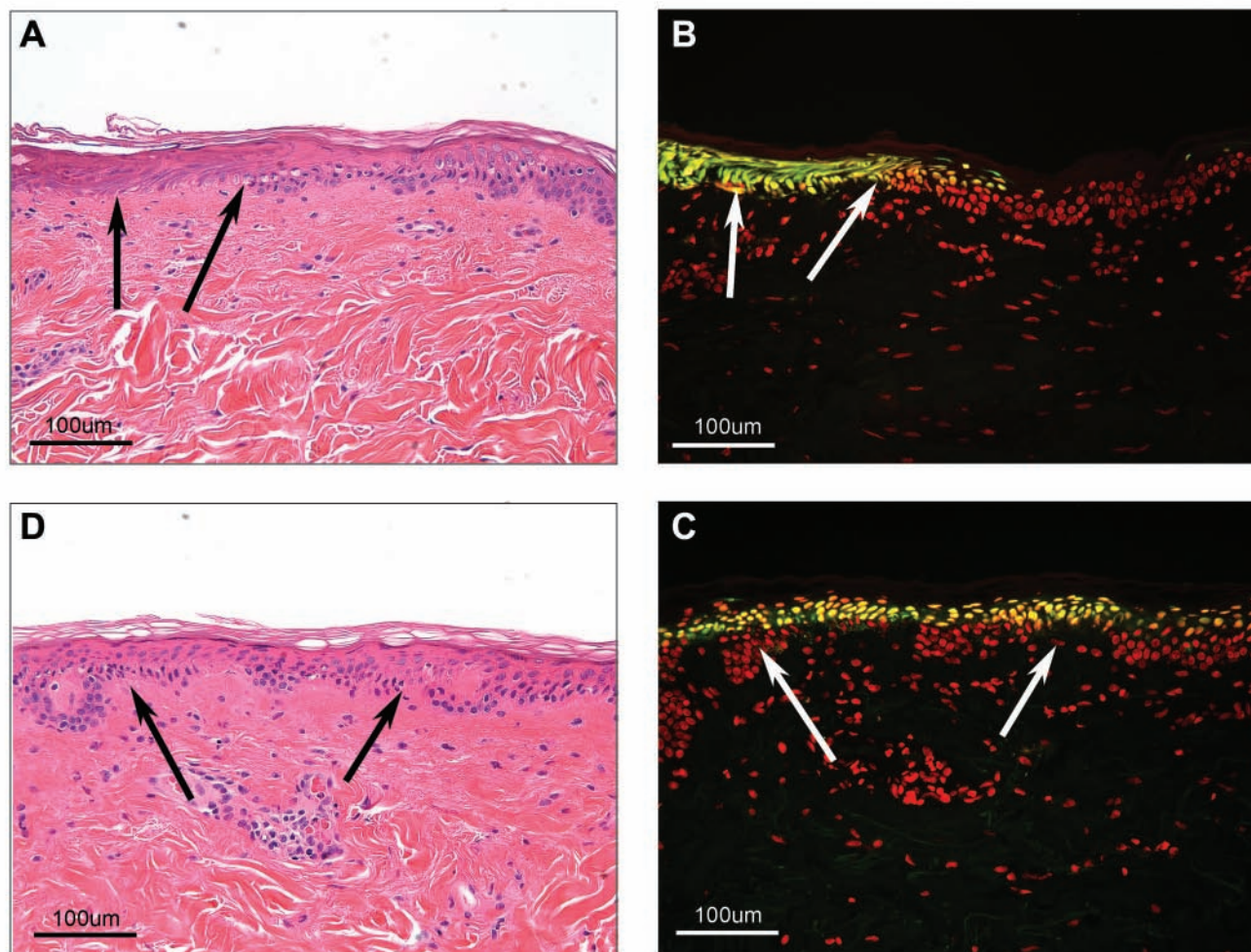


Figure 1. Corresponding hematoxylin and eosin (H&E, A, B) and terminal deoxynucleotidyl transferase-mediated deoxyuridine triphosphate nick-end labeling (TUNEL)-stained (C, D) histological skin sections following treatment with the Active FX system with the same settings (75 mJ/75 Hz) at a density of 2 and 3. Note the bright yellow/orange cells of the epidermis in the TUNEL-stained sections highlighting the affected cells within the treated section. The TUNEL technique allowed for the identification of cellular injury that was imperceptible with standard H&E. Treatments with a density of 1 or 2 demonstrated spacing of the affected areas by intermittent unaffected regions of epidermis. Areas treated with a density ≥ 3 demonstrated affected cells across the length of the entire epidermis in the section. (Magnification $20\times$)

identify irreversible damaged nuclei within the treatment areas.

TUNEL

The assay was performed with the TUNEL kit from Promega Corporation (Madison, Wisconsin).²² Slides were incubated at 56°C for 15 minutes and deparaffinized in xylene, hydrated in graded ethanol solutions, and equilibrated in normal saline for five minutes and then in potassium-phosphate buffer (PBS) concentrate for an additional five minutes. Sections were fixed in 4% paraformaldehyde for 15 minutes and washed in PBS. Sections were then permeabilized with 20 $\mu\text{g}/\text{mL}$ of proteinase K (Promega Corp.) for eight minutes at room temperature

and prepared with 1:500 dilution of 10 mg/mL stock from the kit.

Sections were then washed in PBS and postfixed in 4% paraformaldehyde, washed in PBS again, and equilibrated in 100 μL of equilibration buffer. Slides were then incubated flat in a humid chamber for five to 10 minutes. The terminal deoxynucleotidyl transferase (TdT) reaction mix (45 μL equilibration buffer, 5 μL nucleotide mix, and 1 μL TdT enzyme) was prepared during the equilibration step and protected from light. Then, 50 μL of the TdT reaction mix was applied to each slide. Plastic coverslips were applied before incubating in a humid chamber protected from light for one hour at 37°C . Slides were washed in $2\times$ SSC (Promega Corp.), rinsed and washed in PBS, and

counterstained with propidium iodide (Invitrogen Molecular Probes, Eugene, Oregon). Slides were then washed in double-distilled water and coverslipped with Vectashield.

Fluorescent Microscopy

Slides were evaluated using fluorescence excitation microscopy. TUNEL-positive nuclei demonstrated a bright green fluorescence with the ~ 470 -nm (FITC) fluorescence filter. Mouse thymus was employed as the positive control. Review and photography of all histologic preparations were carried out on a Leica DM2000 photomicroscope (Leica Microsystems, Inc., Bannockburn, Illinois) equipped with bright-field, epifluorescence, and incident angle dark-field illumination. All sections were reviewed with a board-certified pathologist.

The fluorescent photography and measurements were conducted at four times magnification for all specimens. The microcolumns of injury in the skin specimens stained with the fluorescent TUNEL assay were measured with a standardized ocular reticle micrometer by three blinded observers and recorded. The width and depth information was recorded with the assistance of a photosoftware program (Adobe Creative Suite 2, Adobe Systems Incorporated 2007), with a pixel/micrometer ratio of 20:11. Measurements were taken from the most superficial layer of the epidermis to the full depth and/or width of the TUNEL fluorescence. The depth of injury was extrapolated from the nearest area of uninvolved epidermis to the deepest TUNEL-positive cell identified in continuity with the microcolumn of injury. Approximately 60 to 70 microcolumns of injury were measured for each laser parameter.

Statistical Analysis

The deepest and/or widest apoptotic cellular signal identified in continuity with a column of injury at a respective laser parameter was identified and recorded. At least 40 to 45 individual microablation columns were analyzed and recorded at each laser parameter. The depth and width of injury at various clinical energy settings and various numbers of pulses were evaluated. The means and standard deviations were recorded and plotted with a standard software program (Microsoft Excel, 2003).

RESULTS

Following treatment with the Active FX system, H&E-stained sections demonstrated a fractionated pattern of injury along the length the epidermis. The damaged foci were separated by zones of unaffected tissue. The majority of the damage, regardless of energy or pulse width, was localized to the epidermis and superficial papillary dermis.

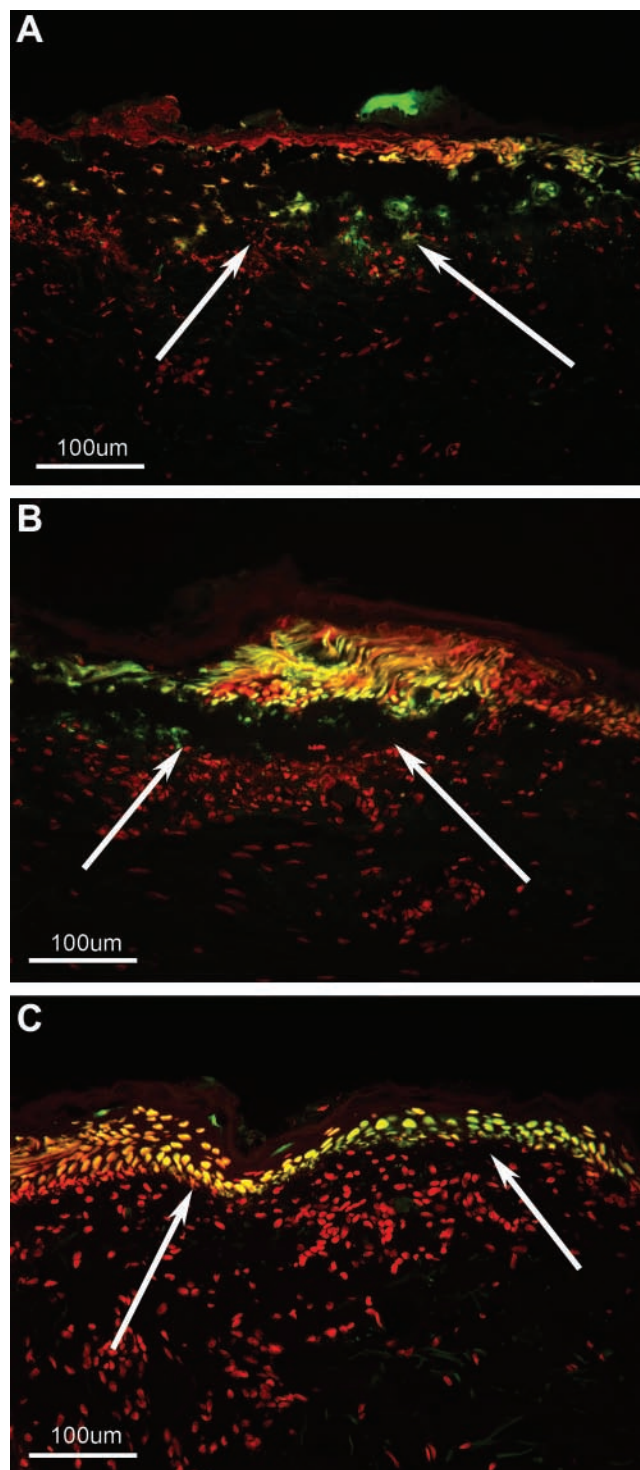


Figure 2. Terminal deoxynucleotidyl transferase-mediated deoxyuridine triphosphate nick-end labeling (TUNEL)-stained histological sections demonstrating the different patterns of injury with a constant energy of 150 mJ at repetition rates of A) 50 Hz, B) 100 Hz, and C) 125 Hz. Note the laser injury becomes more superficial with the faster repetition rates (arrows). (Magnification 20 \times)

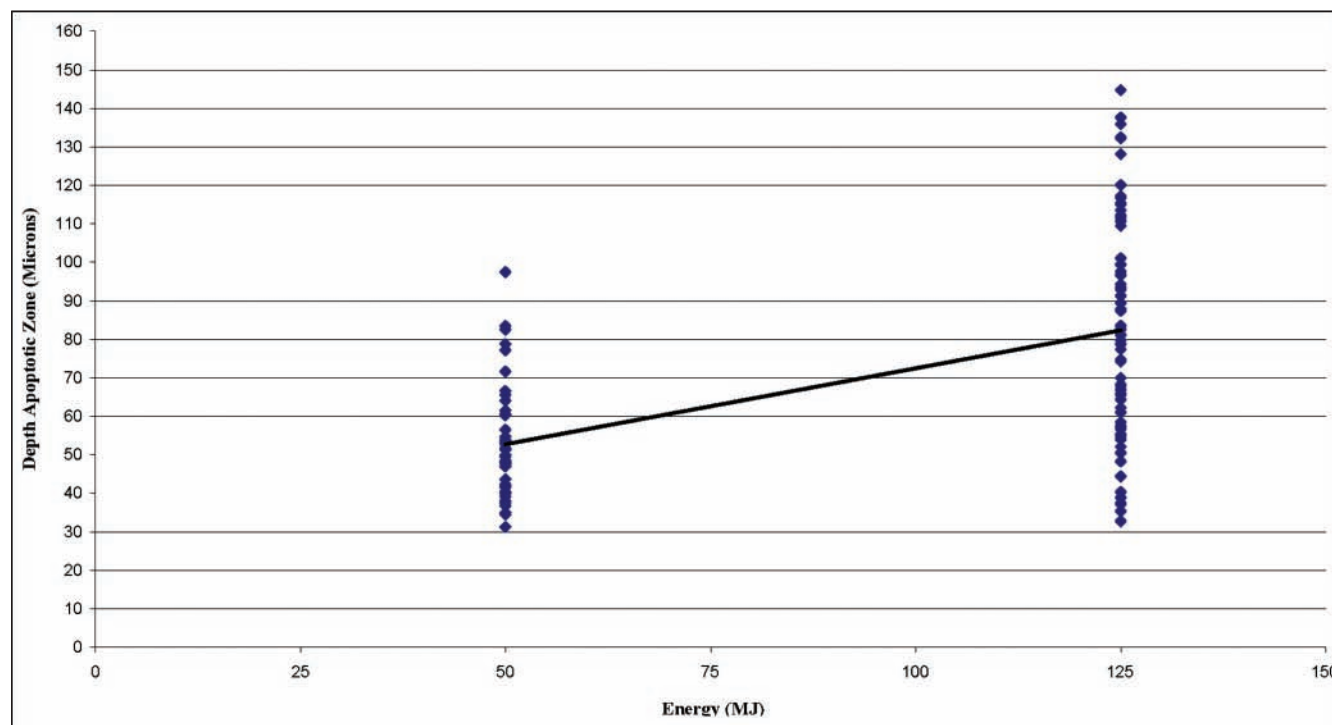


Figure 3. Energy versus depth following treatment with the Active FX system with an equivalent repetition rate (100 Hz).

The superficial craters of ablation were bordered by cells with streamed and fragmented nuclei. In the H&E sections, cells immediately adjacent to the rims of denatured cells maintained their structural integrity and appeared unaltered by the treatment. Higher energy treatments created deeper, wider regions of ablation limited to the epidermis and superficial papillary dermis.

However, in the TUNEL-stained sections (in which sections of irreversibly damaged DNA are labeled), the cells that appeared unaffected in H&E sections demonstrated a positive TUNEL signal, indicating that the cellular injury extended beyond that seen with the H&E sections (Figure 1). Tissue treated with the Active FX at a density of 1 or 2 demonstrated TUNEL-positive nuclei outlining the affected areas separated by regions of TUNEL-negative cells and unaffected tissue. Following a treatment with a density of 3 or greater, regardless of energy or repetition rate, TUNEL-positive nuclei were identified along the entire length of the epidermis.

Damage following treatment with different repetition rates at similar energies was also compared. Slower repetition rate Active FX treatments demonstrated TUNEL-positive nuclei throughout the epidermis and in the papillary dermis. However, following treatments with faster repetition rates, TUNEL-positive nuclei were confined to the superficial epidermis when compared to slower repetition rate treatments (Figure 2). The increased depth of injury associated with the treatments utilizing slower repetition rates was attributed to an increase in

pulse width, which led to an increased dwell or contact time between the energy beam and treatment areas, causing an increased deposition of heat into the treated area. The increased heating and thermal damage resulted in a deeper injury in the skin. The faster repetition rates had shorter pulse widths contributing to less heat deposition into the surrounding treated tissue. The depth of injury with the Active FX system with increasing energy at an equivalent repetition rate (100 Hz) is shown in Figure 3.

In contrast to the Active FX system, following treatment with the Deep FX device, narrow, deep microablation columns were identified in the H&E-stained skin sections (Figure 4). Each of the microcolumns of ablation was surrounded by a rim of coagulated tissue that varied in thickness depending on the parameters of the individual treatment. The microcolumns of ablation were ~125 to 150 μm wide and tapered in a conical fashion from the epidermal surface into the underlying papillary and reticular dermis. The depth of injury was directly related to the energy and number of pulses. Tissue injury was identified up to 4 mm from the epidermal surface with double-pulse treatments at higher energies. The H&E slides gave a much more conservative view of the damage pattern because of the inability to delineate the apoptotic nuclei surrounding the areas of a damage, the true advantage of the TUNEL assay. This was much more obvious and apparent with the specimens following treatment with the Active FX device because of its focus at the hypercellular epidermis and papillary dermis

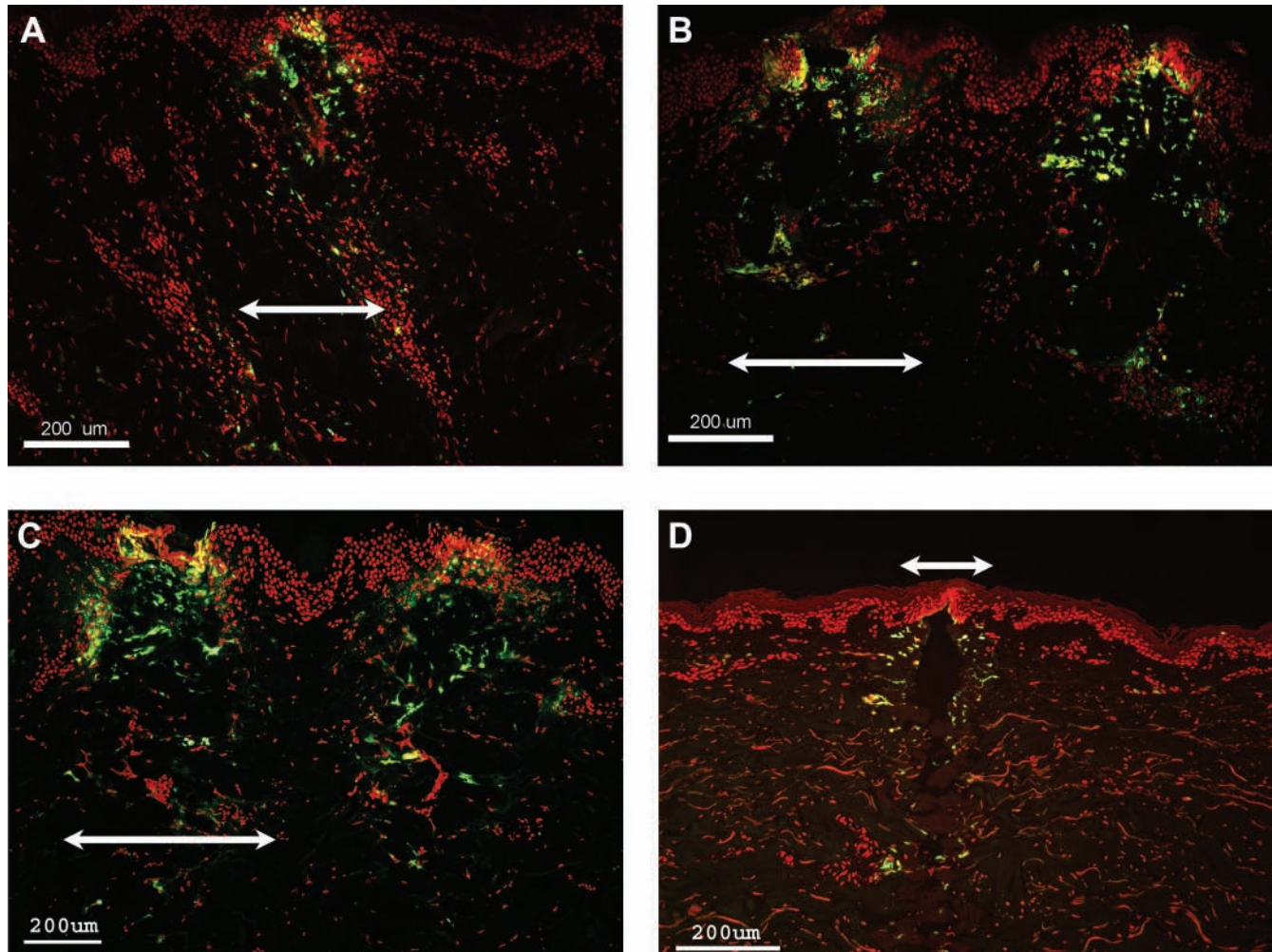


Figure 4. Terminal deoxynucleotidyl transferase-mediated deoxyuridine triphosphate nick-end labeling (TUNEL)-stained histological skin section following treatment with the Deep FX system demonstrating the increase in affected cells surrounding the areas of ablation with increasing fluences and multiple pulsed treatments (15 mJ single (A) and double (B) pulse, 20 mJ single (C) and double (D) pulse; magnification 10x).

compared to the hypocellular deeper reticular dermis. The reason that the same TUNEL positivity is not seen with the Deep FX is due to the increased ablation of the epidermis and papillary dermis. The Deep FX device employs a considerably shorter pulse width, producing more ablation than coagulation and thermal injury as seen with the Active FX device. The increased surrounding TUNEL-positive staining following treatment with the Active FX was attributed to more thermal damage to the hypercellular epidermis and papillary dermis.

The extent of cellular damage was also analyzed with the TUNEL stain. TUNEL-positive cells surrounded the areas of ablation, highlighting the extent of thermal injury beyond the ablation column. Consistent with the H&E sections, with higher energies and multiple pulse treatments, wider and deeper regions of TUNEL-positive cells surrounding the microablation columns were observed. Dermal adnexal structures did not appear to affect the

penetration of the microablation channels. Increased treatment densities resulted in a proportional increase in TUNEL-positive cells between the microcolumns of ablation. At a density greater than or equal to 4, TUNEL-positive cells were identified across the entire tissue plane with minimal to no separation between the columns of injury (Figure 5). With the apoptotic/necrotic cellular signal as our marker, depth of tissue injury was measured for 5, 10, 15, and 20 mJ with single- and double-pulsed treatments (Figure 6A,B). The difference in the width of injury with multiple pulsed treatments was evaluated at clinical fluences of 10 and 15 mJ (Figure 7A,B).

The total damage pattern of the combination treatments was consistent with the pattern observed with each device alone. With standard H&E staining, the sections treated with both the Active and Deep FX systems in combination showed the broad-based fractionated epidermal injury typical of the Active FX superimposed with the deep

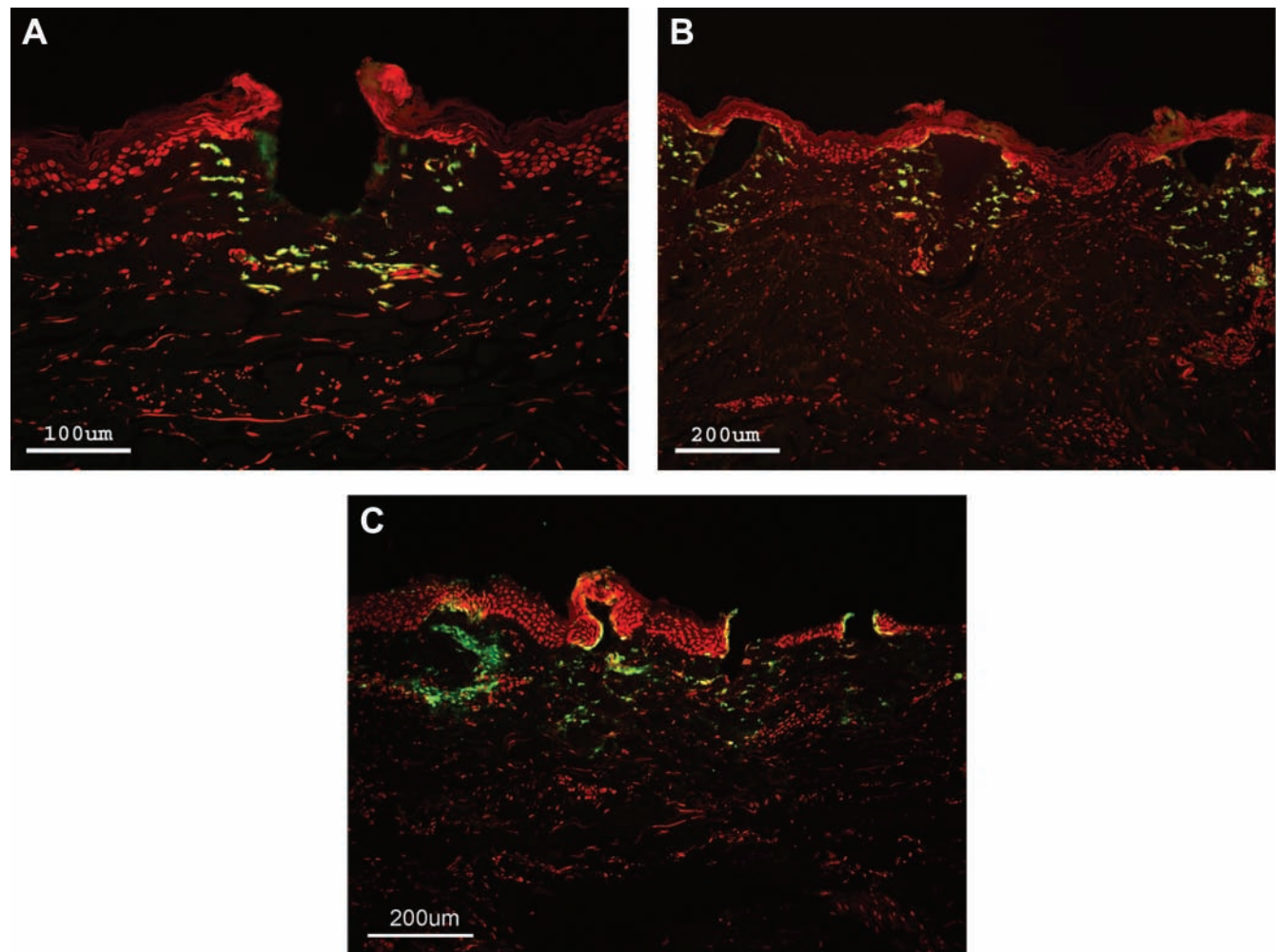


Figure 5. Terminal deoxynucleotidyl transferase-mediated deoxyuridine triphosphate nick-end labeling (TUNEL)-stained histological skin section following a single pulsed treatment with the Deep FX device with changes in density of 1 (A), 3 (B), and 5 (C) at a constant energy (5 mJ). At a density ≥ 4 , TUNEL-positive cells were identified almost homogeneously across the section demonstrating thermal injury in the dermis extending from one microablation column to the next adjacent microcolumn. Notice the fractional ablative injury in the epidermis and the wider thermal injury highlighted by the TUNEL-stained nuclei in the papillary and reticular dermis. (Magnification $20\times$, $10\times$, $10\times$)

microcolumns of ablation penetrating into the underlying papillary and reticular dermis produced by the Deep FX treatment. The TUNEL stain demonstrated the epidermal damage consistent with the Active FX pattern of injury, combined with the intermittent deep injury columns of the Deep FX treatment.

DISCUSSION

The concept of fractional photothermolysis and fractional ablation has revived the interest in carbon dioxide laser resurfacing and has become an attractive option to many laser surgeons.^{18-20,23-26} Nevertheless, clinical application of these novel ablative fractional technologies has, once again,

preceded any solid scientific validation. In the past, the conventional carbon dioxide devices were limited by the degree of residual thermal damage following treatment increasing the risk of hypopigmentation and a prolonged recovery. The heating component of the carbon dioxide laser is thought to be the major cause of the comorbidity and downtime observed with the older, conventional CO₂ resurfacing. However, with the adjustable densities, pulse widths, and energies, one can potentially control the degree of coagulation, ablation, and depth for a given treatment area and/or site while minimizing the downtime and potential comorbidities seen with older traditional resurfacing. The optimal distance between ablation columns, amount of ablation versus coagulation, depth of treatment, or density of the number of the microablative/thermal columns in a given

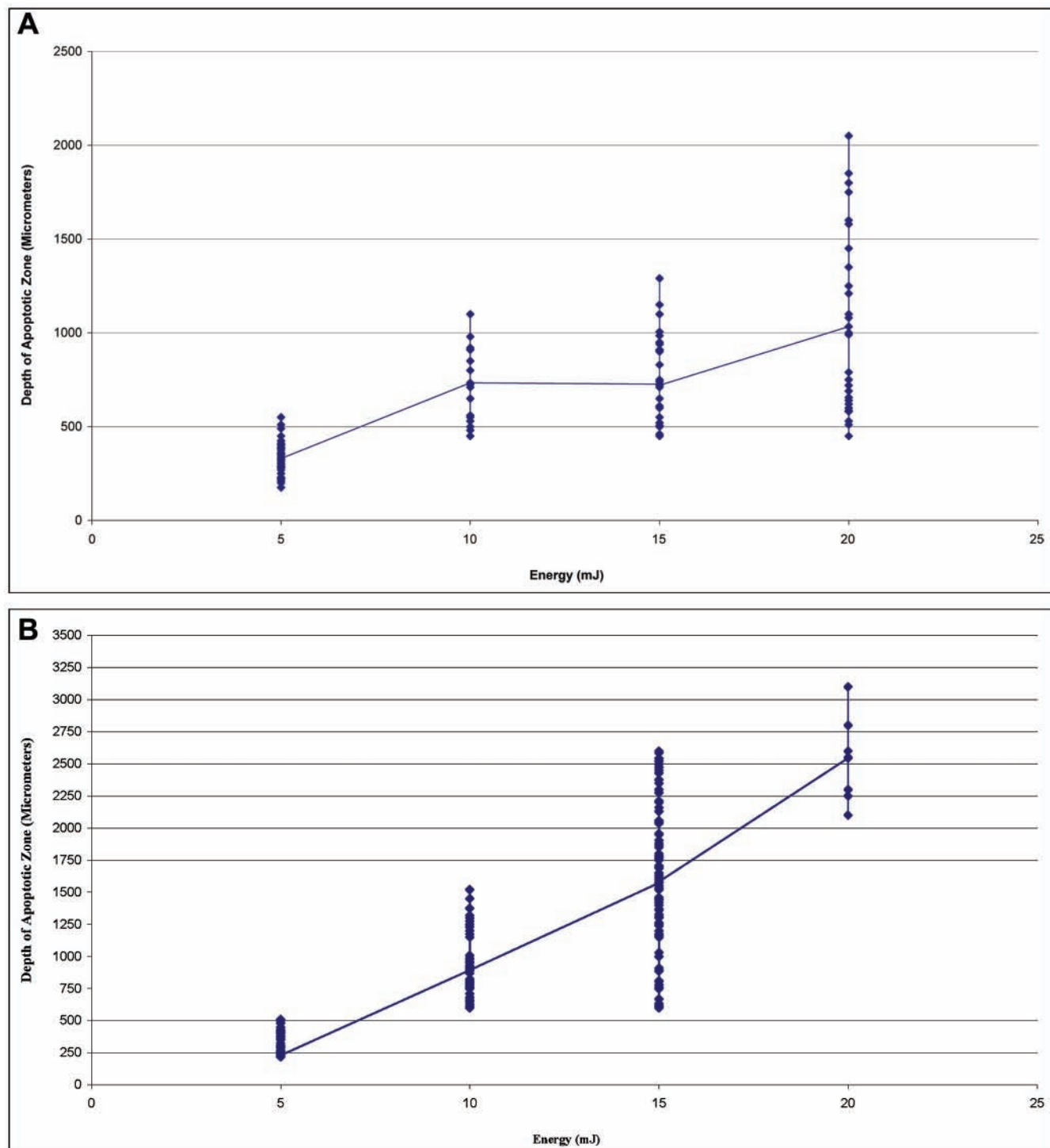


Figure 6. Depth of tissue injury following single pulse (A) and double pulse (B) treatments.

region to maximize neocollagenesis and stimulate wound healing is still yet to be fully understood.

The acute histopathological damage profile following treatment with the Active FX and Deep FX was dependent on energy, repetition rate, number of pulses, and density. The Active FX system produced a broad-based

superficial pattern of ablation that was limited to the epidermis and superficial papillary dermis. The Active FX device employs a pulse width that is eight to 10 times longer than that of the Deep FX device, with a much larger spot size (1.2 mm vs 125 μ m). The Deep FX device has the potential to extend treatment from the epidermis

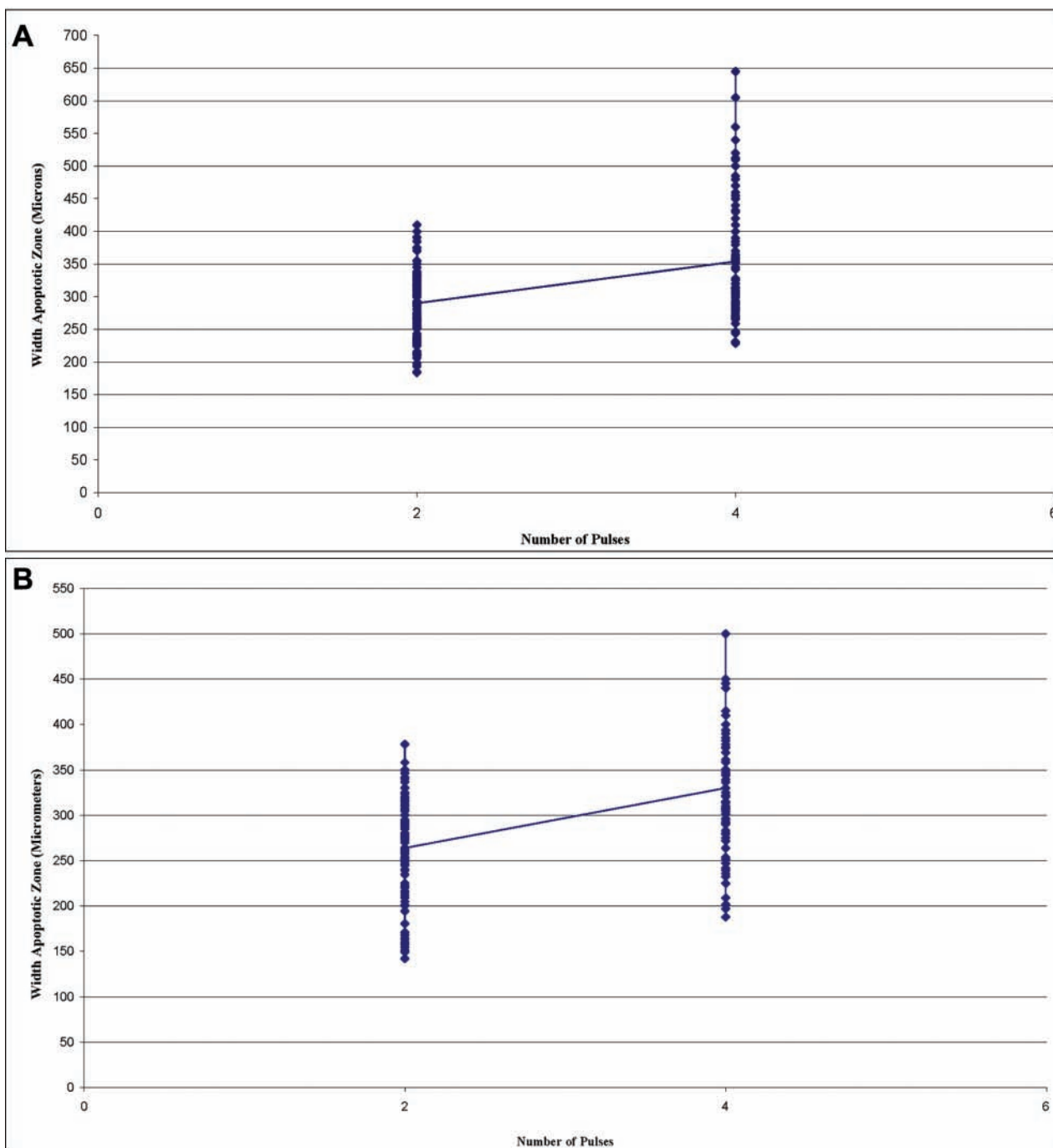


Figure 7. Width of injury following Deep FX treatment at 10 mJ (A) and 15 mJ (B).

to as deep as 3 to 4 mm into the reticular dermis. The fractional Deep FX CO₂ device utilizes a shortened pulse width with a smaller (125 μ m) spot size, which allows for deep tissue ablation/penetration. By manipulating the number of pulses, density, and energy per pulse, the degree of thermal injury to the tissue can be controlled. On account of the long pulse width and large spot size, the Active FX does not have the capability of the deeper

tissue penetration demonstrated with the Deep FX device. Clinically, this information has been very helpful in developing understanding of the technology and has also assisted in providing the appropriate treatment plan to achieve certain treatment goals. For example, in a patient with deep rhytids or ice pick acne scars, the Active FX is more suitable for a superficial blending of the epidermis and superficial dermis, but this would not address the

deeper rhytids that would be more amenable to a Deep FX treatment. This histopathological mapping of injury with TUNEL was also helpful in tailoring laser skin resurfacing treatment plans for different regions of the face and understanding the extent of total tissue affected for a given treatment. For example, generally, a more aggressive deeper treatment is necessary for areas such as the perioral region (where the skin is thicker and denser), whereas areas such as the lid/cheek junction are considerably thinner with more fragile tissue, and a more superficial treatment is more appropriate.

The TUNEL histology has improved our understanding of the extent of acute damage with the individual treatments, which was not observed with standard H&E alone. Clinical studies evaluating optimal treatment densities, energies per pulse, and number of pulses for each of the devices alone and in combination are currently under way. The histological damage profiling of laser/tissue interaction with the TUNEL assay provides insight into the aggressiveness of each treatment and the extent of the actual overall acute tissue damage of both ablative and thermal injury detail, which is not provided with standard H&E staining. The TUNEL stain identifies irreversibly damaged nuclei, so treatments that encompass areas that have a higher cellular content such as the epidermis, papillary dermis, and/or dermal appendages highlight areas of injury at a greater extent than hypocellular areas. Therefore, injury within treatment areas with higher cellular content was more easily identified than in more hypocellular areas, such as the reticular dermis.

Our study is not without limitations. We emphasize that the acute histopathological changes illustrated in this report only provide information on the immediate tissue response following treatment with these two devices and is not a clinical report. Clinically, resurfacing procedures are performed on facial or neck skin, not on abdominal skin. Facial skin is densely populated with hair follicles, sebaceous glands, and blood vessels. Therefore, facial skin may react differently to the laser treatment than human abdominal skin. Also, it is important to note the thickness of the abdominal skin examined in this study, which was more than 5 to 6 mm thick. Facial skin is significantly thinner, which should be considered when planning laser treatments at aggressive energy settings.

Besides the anatomic tissue differences, there are inherent obstacles that must be taken into account when evaluating laser skin interactions histologically. Due to processing and microtome sectioning, precise tissue measurements following the laser treatment may not be a true representation of the actual tissue injury in vivo. Paraffin-embedded tissue sections require dehydration of the tissue samples, which causes shrinkage. This is an important point to consider when evaluating microcolumn lesion depth and width.^{19,20} Also, due to the conical shape of the laser injury, slight sectioning angles may dramatically affect the identification of the true depth of a microcolumn. To overcome this problem, multiple serial

sections were cut, numerous columns were measured, and treatments were performed in at least triplicate to provide an accurate representation of the tissue injury at a given treatment parameter. Along with H&E staining, the TUNEL method was a helpful adjunct in evaluating the extent of injury on account of its ability to label the irreversibly damaged cells surrounding the area of injury.^{21,22,27-29} However, keratinocytes of the epidermis and fibroblasts within or surrounding an obvious area of injury did not always fluoresce with the TUNEL-positive signal. Natural thermal tolerance from cell to cell, as well as complete denaturation and destruction of chromosomes, should be taken into account when viewing the TUNEL-stained sections.

CONCLUSIONS

This is the first report of the acute histopathological characterization of the laser-induced injury to human skin in vivo following treatment with the Active and Deep FX short-pulsed CO₂ devices in the literature. This side-by-side acute histopathological comparison helps clinicians to understand the differences between these two novel technologies and provides the first step in understanding tissue response following treatment with these devices in an in vivo human model. Evaluating the skin response following treatment with the various laser settings over the wound-healing period is critical to fully understand the laser tissue dynamics and biologic processes that are intricately involved in the laser tissue interaction.

Disclosures and Funding

The devices in the study were donated for research purposes by Lumenis Ltd, but no other financial support was provided for the study. None of the authors declared any personal conflicts of interest with regard to the authorship or publication of this article.

REFERENCES

1. Trelles MA, Rigau J, Mellor TK, et al. A clinical and histological comparison of flashscanning versus pulsed technology in carbon dioxide laser facial skin resurfacing. *Dermatol Surg* 1998;24:43-49.
2. Taub AF. Fractionated delivery systems for difficult to treat clinical applications: acne scarring, melasma, atrophic scarring, striae distensae, and deep rhytides. *J Drugs Dermatol* 2007;6:1120-1128.
3. Tanzi EL, Alster TS. Single-pass carbon dioxide versus multiple-pass Er:YAG laser skin resurfacing: a comparison of postoperative wound healing and side-effect rates. *Dermatol Surg* 2003;29:80-84.
4. Seckel BR, Younai S, Wang KK. Skin tightening effects of the ultrapulse CO₂ laser. *Plast Reconstr Surg* 1998;102:872-877.

5. Schwartz RJ, Burns AJ, Rohrich RJ, et al. Long-term assessment of CO₂ facial laser resurfacing: aesthetic results and complications. *Plast Reconstr Surg* 1999;103:592-601.
6. Ross EV, Grossman MC, Duke D, et al. Long-term results after CO₂ laser skin resurfacing: a comparison of scanned and pulsed systems. *J Am Acad Dermatol* 1997;37:709-718.
7. Goldman MP, Marchell N, Fitzpatrick RE. Laser skin resurfacing of the face with a combined CO₂/Er:YAG laser. *Dermatol Surg* 2000;26:102-104.
8. Fitzpatrick RE. CO₂ laser resurfacing. *Dermatol Clin* 2001;19: 443-451, viii.
9. Duke D, Khatri K, Grevelink JM, et al. Comparative clinical trial of 2 carbon dioxide resurfacing lasers with varying pulse durations: 100 microseconds vs 1 millisecond. *Arch Dermatol* 1998;134:1240-1246.
10. Apfelberg DB, Smoller B. UltraPulse carbon dioxide laser with CPG scanner for deepithelialization: clinical and histologic study. *Plast Reconstr Surg* 1997;99:2089-2094.
11. Burkhardt BR, Maw R. Are more passes better? Safety versus efficacy with the pulsed CO₂ laser. *Plast Reconstr Surg* 1997;100:1531-1534.
12. Dierickx CC, Casparian JM, Venugopalan V, et al. Thermal relaxation of port-wine stain vessels probed in vivo: the need for 1-10-millisecond laser pulse treatment. *J Invest Dermatol* 1995;105:709-714.
13. Fitzpatrick RE, Rostan EF, Marchell N. Collagen tightening induced by carbon dioxide laser versus erbium: YAG laser. *Lasers Surg Med* 2000;27:395-403.
14. Trelles MA, David LM, Rigau J. Penetration depth of Ultrapulse carbon dioxide laser in human skin. *Dermatol Surg* 1996;22:863-865.
15. Trelles MA, Garcia L, Rigau J, et al. Pulsed and scanned carbon dioxide laser resurfacing 2 years after treatment: comparison by means of scanning electron microscopy. *Plast Reconstr Surg* 2003;111:2069-2078; discussion 2079-2081.
16. Walsh JT, Jr., , Deutsch TF. Pulsed CO₂ laser tissue ablation: measurement of the ablation rate. *Lasers Surg Med* 1988;8:264-275.
17. Walsh JT, Jr., , Deutsch TF. Pulsed CO₂ laser ablation of tissue: effect of mechanical properties. *IEEE Trans Biomed Eng* 1989;36:1195-1201.
18. Manstein D, Herron GS, Sink RK, et al. Fractional photothermolysis: a new concept for cutaneous remodeling using microscopic patterns of thermal injury. *Lasers Surg Med* 2004;34:426-438.
19. Hantash BM, Bedi VP, Kapadia B, et al. In vivo histological evaluation of a novel ablative fractional resurfacing device. *Lasers Surg Med* 2007;39:96-107.
20. Hantash BM, Bedi VP, Chan KF, et al. Ex vivo histological characterization of a novel ablative fractional resurfacing device. *Lasers Surg Med* 2007;39:87-95.
21. Farkas JP, Richardson JA, Hoopman JE, et al. TUNEL assay for histopathologic evaluation of irreversible chromosomal damage following nonablative fractional photothermolysis. *Plast Reconstr Surg* 2008;122: 1660-1668.
22. Gavrieli Y, Sherman Y, Ben-Sasson SA. Identification of programmed cell death in situ via specific labeling of nuclear DNA fragmentation. *J Cell Biol* 1992;119: 493-501.
23. Geronemus RG. Fractional photothermolysis: current and future applications. *Lasers Surg Med* 2006;38: 169-176.
24. Fisher GH, Geronemus RG. Short-term side effects of fractional photothermolysis. *Dermatol Surg* 2005;31:1245-1249; discussion 1249.
25. Graber EM, Tanzi EL, Alster TS. Side effects and complications of fractional laser photothermolysis: experience with 961 treatments. *Dermatol Surg* 2008;34: 301-305; discussion 305-307.
26. Tanzi EL, Wanitphakdeedecha R, Alster TS. Fraxel laser indications and long-term follow-up. *Aesthetic Surg J* 2008;28:675-678; discussion 679-680.
27. Nakaseko H, Kobayashi M, Akita Y, et al. Histological changes and involvement of apoptosis after photodynamic therapy for actinic keratoses. *Br J Dermatol* 2003;148:122-127.
28. Okamoto H, Mizuno K, Itoh T, et al. Evaluation of apoptotic cells induced by ultraviolet light B radiation in epidermal sheets stained by the TUNEL technique. *J Invest Dermatol* 1999;113:802-807.
29. Raskin CA. Apoptosis and cutaneous biology. *J Am Acad Dermatol* 1997;36:885-896; quiz 897-898.